

Investigation of Leakage and Transmission Radiation through the MLC Version I2 Applied To the Elekta Synergy 6 MV Photon Beam Linac

Deae-Eddine Krim^{1*}, Dikra Bakari², Mustapha Zerfaoui¹, Abdeslem Rrhioua¹, Mohammed Hamal¹, Khalid El Ouardy¹

1. LPMR, Faculty of sciences, University Mohamed 1st, Oujda, Morocco.
2. National School of Applied Sciences, University Mohamed 1st, Oujda, Morocco.

ARTICLE INFO	ABSTRACT
Article type: Original Paper	Introduction: Radiotherapy and nuclear medicine extensively use Monte Carlo simulation to study particle transport and interactions. The aim of this task is the investigation and simulation of leakage and transmission (L&T) particles using the Multi-Leaf Collimator version i2 applied to the Elekta Synergy linac.
Article history: Received: Dec 23, 2021 Accepted: Apr 05, 2022	Material and Methods: In this study, all linac segments are included in the simulation model. In order to reduce MC calculation time, the new HPC-Slurm cluster platform and the Python phase space approach are used. To study the transmission between MLCi2 leaves, a detailed analysis of the dose distribution was conducted.
Keywords: Radiotherapy Monte Carlo Multi-Leaf Collimator MLCi2 Leakage and Transmission L&T	Results: The simulation results obtained with Gate 9.0 MC are excellently correlated with the measured data with error estimates for the 6 MV photon beam parameters less than 1% and a validation level of 99% in terms of the gamma index's (2%/2mm) threshold formalism for the cross profiles and PDD's dose distributions. The results indicate that contamination particles (e-, e+) have an effect on the distribution of dose in the patient. These particles are present in the beam produced previously and which is assumed to contain only X-rays. In addition, a three-dimensional distribution of dose inside the tumor (CT-scan) confirms the L&T effect of the studied version of the multi leaf collimator (MLCi2), with a dose range of around 70% of the delivered dose to the tumor, resulting in secondary outcomes at the DNA. Conclusion: Consequently, the production of a new generation of MLC that can limit this L&T effect should be encouraged.

► Please cite this article as:

Krim DE, Bakari D, Zerfaoui M, Rrhioua A, Hamal M, El Ouardy Kh. Investigation of Leakage and Transmission Radiation through the MLC Version I2 Applied To the Elekta Synergy 6 MV Photon Beam Linac. Iran J Med Phys 2022; 19: 334-345. 10.22038/IJMP.2022.62432.2055.

Introduction

The Monte Carlo (MC) methodology is one of the most impressive techniques used to model particle interaction and transport in many different domains (medical physics, astronomy, etc.) [1]. Over the previous five decades, the scientific community has extensively used MC algorithms, particularly in radiation treatment [2-3]. Consequently, several researchers have employed MC approaches to effectively examine patient dosage delivery [4]. The Multi-Leaf Collimator (MLC), on the other hand, is an essential device for linacs. Whereas, the main objective of radiation oncology physics is to have a complete understanding of MLC mechanics and dosimetric characteristics. It is currently widely used in a three-dimensional Conformal Radiation Therapy (3D-CRT) and Intensity-Modulated Radiation Therapy (IMRT). Furthermore, MLC is often employed to produce irregular fields depending on the mobility of the leaves [5-7].

In clinical treatments, a sufficient distance should be provided between adjacent leaves to ensure that each MLC leaf moves freely and flexibly to avoid leaf deformation and stickiness during movement. However, a field-shape construction must be created on the leaf's side to prevent radiation leakage, and the leakage between adjacent leaves is eliminated using a tongue-and-groove (T&G) design. As a result, the MLC leaves may move regularly and dependably. When small and complex tumors are treated, the Monitor Unit (MU) used for a single plan irradiation may reach up to 1000 MU, resulting in a significant MLC leakage impact on the target volume and normal tissues, requiring quantitative assessment. There are several common methods that have been proposed in the literature to investigate the leakage of prior generations of MLC systems in order to decrease and eliminate this impact. Kim et al. [5] and Mark et al. [6] investigate radiation transport through MLC and calculate MLC transmission and scatter for dynamic

*Corresponding Author: Tel: +212 636 866 627; Email: d.krim@ump.ac.ma

IMRT, respectively. Also, Li et al. [7] examined the clinical feasibility of leakage and transmission radiation dosimetry caused by gravity on the ELEKTA Synergy-S linac's MLC system. All these studies are done to stimulate the vendor to improve a new generation of MLC models without leakages. For that purpose, the MLC version i2 presents one of the latest versions of MLC developed by the company Elekta (Elekta AB, Stockholm, Sweden), and to our knowledge, this version has never been evaluated in terms of leakage and transmission in the literature. To this end, the present paper includes an examination of the MLC version i2 applied to model volumetric modulated arc therapy (VMAT) and IMRT treatments. All used steps in simulation strategy of the independent and dependent patient parts of Elekta Synergy MLCi2 linac are fully described. The simulated PDD's and cross-profile dose distributions using the last version of HPC-SLURM-cluster are compared with experimental data. Furthermore, the impact of each segment on the X-ray beam and the L&T radiation through MLC version i2 is being investigated.

Materials and Methods

Implementation of Elekta Synergy MLCi2 linac geometry

The Elekta Synergy MLCi2 linac platform (Elekta company, stockholm, Sweden), which delivers the energy photon beam (X-ray-6 MV) with a suggested dose rate of 400 MU/min, was used in this study. The experiment data are collected using a Scanditronix Wellhofer CC13 cylindrical ionization chamber with an

active volume of 0.13 cm³ mounted over a motorized guide in an IBA Blue Phantom (IBA dosimetry, Schwarzenbruck, Germany) resistance temperature detector [8]; all experiment quantities are measured using the AAPM's TG-51 methodology [9]. The open-source platforms: VV created for editing and recording 4D CT scans, ROOT object-oriented version 6.14 developed by CERN collaboration, and GEANT4 Application for Emission Tomography (GATE) MC code version 9.0 (Feb. 2020), are utilized. Furthermore, the GEANT4 QT User Interface is used to verify and display the component geometry and overlaps across graphical interfaces [12].

Count on the information of the Elekta Synergy MLCi2 linac segment sizes and shapes shown in the latest papers published in the literature [10]; the linear accelerator components are modelled using the Gate 9.0 MC code. Additionally, Figure 1 (a) shows the general structures of the approach used to model the linear accelerator; this research also takes into account the water phantom.

Simulation components shown in Figure 1 (a) can be summarized as follow (Table 1).

- Elekta Synergy linac Independent Patient Part: This particular part of Elekta Synergy MLCi2 linac describes the simulation of the unchangeable components, including the X-ray target, primary collimator, flattening filter F.F, ionizing chamber, back-scatter plate, and finally, the mylar mirror (Figure 1. (a)).

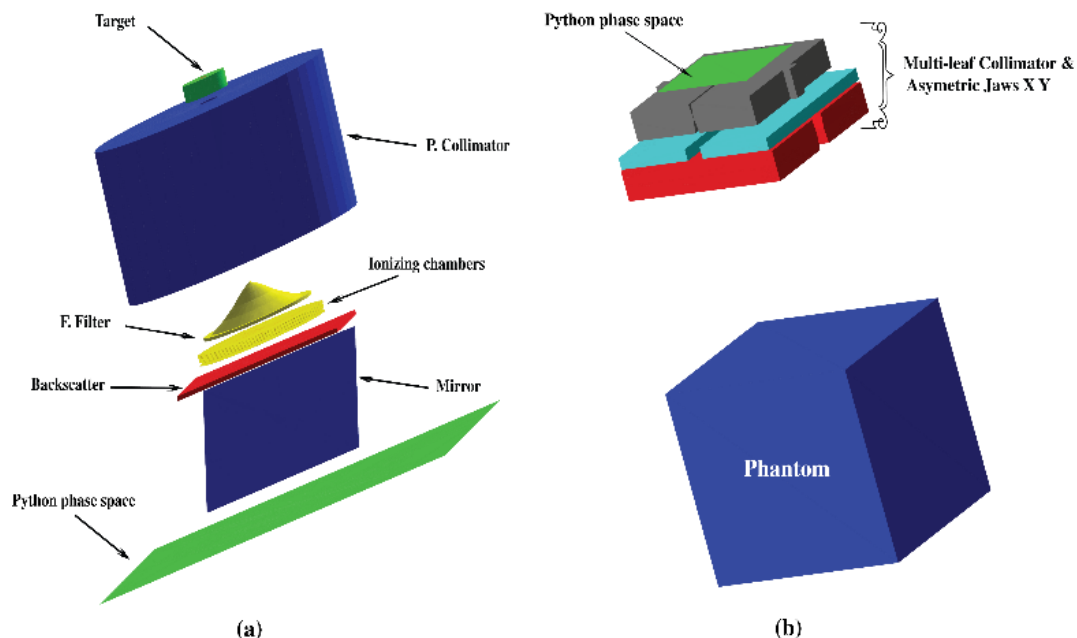


Figure 1. The geometry of the Elekta Synergy MLCi2 system components modeled using the MC Gate 9.0 simulation.

Table 1. The structural configuration of linac modeling converted on MC Gate 9.0

	Linac component		Converted structure Gate 9.0 version
Elekta Synergy linac Independent Patient Part	X-ray target	—————	Insert Cylinder (Green cylinder)
	Primary collimator	—————	Insert Cone (Blue cone)
	Flattening filter	Python Ph. Sp	Insert Cone (Yellow cones)
	Ionizing chambers	—————	Insert Cylinder (Yellow cylinders)
	Back-scatter plate	—————	Insert Box (Red box)
	Mylar mirror	—————	Insert Box (Blue box)
Elekta Synergy linac dependent Patient Part	Multi-leaf Collimator	—————	Insert Trapezoid Box, part of Circle
	Asymmetric jaws X and Y	—————	Insert Trapezoid Box, part of Circle
	Phantom	—————	Insert Box

- Python phase space: According to the Elekta Synergy linac independent patient part components description, these linac section components are never changed during a real treatment. For that purpose, the approach based on the Python phase space is used to record millions of particles by simulating the Elekta Synergy linac Independent Patient Part. So, the Python phase space is built once and used for all size fields to minimize the time calculation.
- Multi-Leaf Collimator MLCi2: The tungsten alloy composition, the rounded portion, and the T&G (Tongue and Groove) form were all described as physical properties of the MLC version i2 Leafs.
- Secondary collimators X, Y: Secondary collimators X, Y are constructed of tungsten alloy, approximately 10 cm in thickness, and have a rounded section in the end of each jaw.
 - Phantom: Box of water with size $50 \times 50 \times 50$ cm³, covered by 1 cm of plastic outer, located at an SSD = 100 cm from the target.

Simulation techniques

Regarding the Elekta Synergy linac simulation, the primary and secondary particles (X-ray, e-, and e+) generated have a range of megavoltage energies. The Electromagnetic Standard Option 3 library's physics processes (EM standard opt3) [10] are used to manage the generated primary and secondary particles with a step limiter of 1 mm over the water box phantom, which corresponds to energy cuts of approximately 350 keV for both electrons and positrons, and 5 keV for photons. The full width at half maximum (FWHM) and the mean energy are used to determine the primary electron source characteristics. Additionally, to adjust the mean energy of the primary electron beam, the administered doses that are produced by a number of simulations run with a total of ten billion (10^{10}) primary electrons are compared to standard measures, taking into account energy ranging from 5 to 7 MeV with a growth step of 0.1 MeV. As a consequence, the mean energy (6.7 MeV), the FWHM energy is fixed to 3% of the mean energy (0.207 MeV), and the FWHM (3 mm) was determined to be the best fit for this Elekta Synergy MLCi2 model simulation.

Furthermore, the used strategy in this simulation to investigate contamination particles can be summarized in two steps.

Python phase space method

- The initial Python phase-space is positioned under the last component of the I.P.P (Mirror). This phase space presents a Variance Reduction Technique (VRT) applied method to reduce MC time simulation.
- The second phase-space is placed under the initial VRT phase space, managed to analyze particles' distribution before any interactions with the variant portion (MLCi2 and Jaws XY) of linac.
- The last phase-space is located below the MLC; it exhibits the distribution of L&T particles generated and crossing through the MLC version i2.

Dose calculation and efficiency:
- Comparisons are made between the MC Gate simulation and experiment dose distributions for the photon beam Elekta Synergy MLCi2 linac using a number of dose metrics. Where the following statistical differences are utilized: The global gamma index ϵ will tend to be accurate in higher dose gradient locations, with a passing rate of only 3%. Failures in high and low dose gradients are shown by the local (γ) and global (ϵ_{\max}) gamma indices, which are normalized to the maximum value of the measured data [13-14].
- Openmosix cluster program of the latest version of cluster computing HPC-Slurm (Slurm - CNRST Team – Morocco) is utilized to split the main code Gate into 1000 sub-task running on 80 CPU (Multiprocessing mode) [15-18].

Results

Statistical dose validation

To assess the simulation of the Elekta Synergy linac in terms of beam quality and field size effects, the dose test evaluation was carried out on four square radiation fields of various sizes. The percentage depth doses PDD's and cross-profiles are displayed (Figure 2) and compared (Table 2) to the reference dose at depths d_{\max} , 5 cm, 10 cm, and 20 cm. Furthermore, Table 3 shows the comparison of the TPR index, output factors OFs, D_{10} (%), d_{\max} (cm), and $d_{80\%}$ (cm) parameters in water for all square fields ranging from 3×3 to 20×20 cm². The comparisons were done according to international guidelines (IAEA TRS 398).

It enables precise authentication of the photon beam's quality [19]. The dissimilarity between the results from the MC Gate simulation and experiment at this comparison, as shown in Table 3, is less than 1.54%.

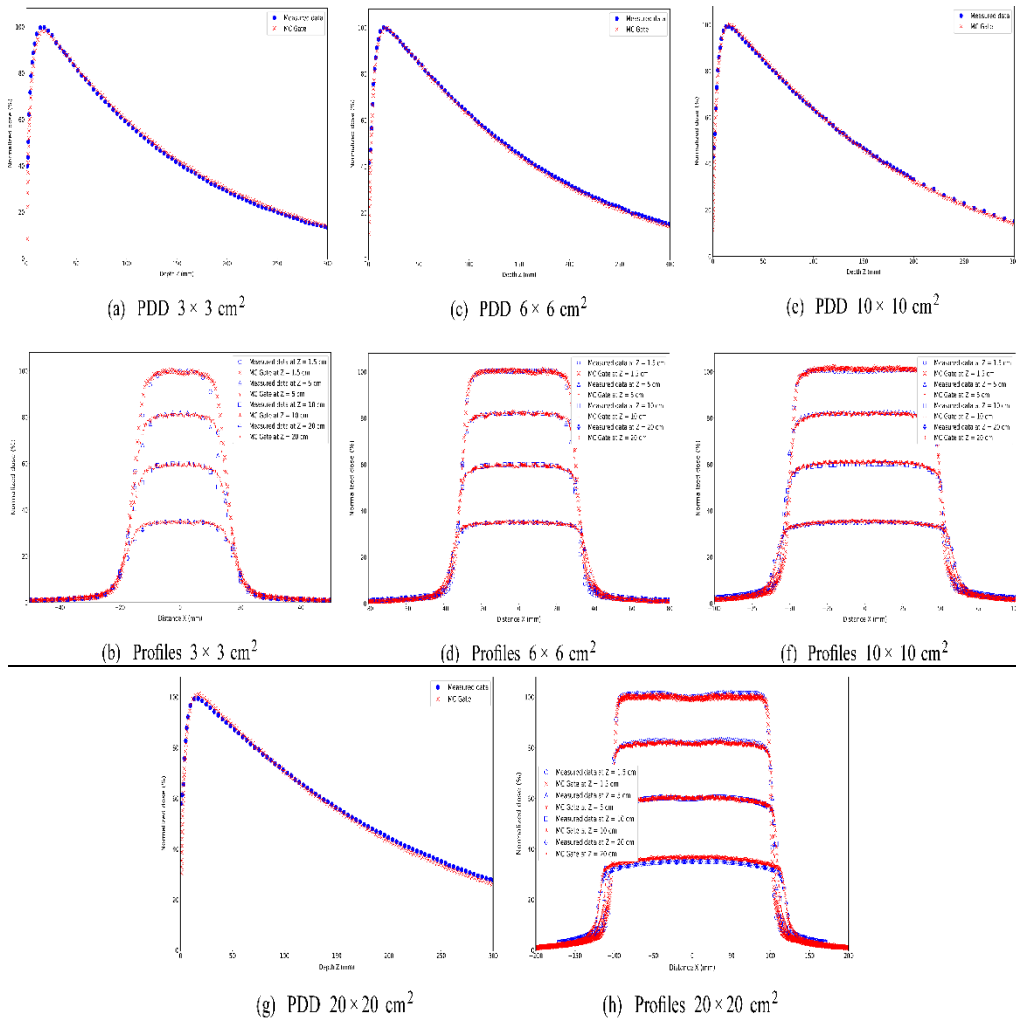


Figure 2. Comparison of simulated and measured PDD's and cross profiles for field sizes ranging from 3×3 to 20×20 cm² for Elekta Synergy MLCi2 linac.

Table 2. Dose index analysis, percentage of points passing the criteria 2%/2mm, 3%/2mm, ϵ and ϵ_{max} for PDD and profiles at four depths d_{max} , 5, 10 and 20 cm for four different fields.

Field (cm ²)	Depth (cm)	ϵ	ϵ_{max}	$\gamma(2\%/2mm)$	$\gamma(3\%/2mm)$
3x3	PDD	9.25×10^{-5}	1.82×10^{-5}	99.5935	100
	d_{max}	9.17×10^{-3}	1.99×10^{-3}	100	100
	5	1.05×10^{-2}	2.94×10^{-3}	98.2906	100
	10	6.90×10^{-3}	1.94×10^{-4}	99.1525	100
	20	7.10×10^{-3}	1.46×10^{-3}	99.154	100
6x6	PDD	1.07×10^{-3}	2.32×10^{-5}	99.187	100
	d_{max}	4.38×10^{-3}	6.86×10^{-4}	98.2456	100
	5	6.22×10^{-3}	1.11×10^{-3}	100	100
	10	3.69×10^{-3}	7.15×10^{-3}	100	100
	20	4.53×10^{-3}	1.13×10^{-3}	100	100
10x10	PDD	9.42×10^{-4}	6.15×10^{-4}	99.537	100
	d_{max}	4.30×10^{-3}	9.18×10^{-4}	100	100
	5	5.03×10^{-3}	8.74×10^{-4}	99.1796	100
	10	4.28×10^{-3}	1.00×10^{-3}	99.1597	100
	20	2.82×10^{-3}	1.03×10^{-3}	100	100
20x20	PDD	1.66×10^{-3}	1.01×10^{-3}	99.124	100
	d_{max}	3.67×10^{-3}	1.87×10^{-3}	99.2701	100
	5	2.89×10^{-3}	7.15×10^{-4}	100	100
	10	2.26×10^{-3}	7.47×10^{-4}	99.2701	100
	20	1.82×10^{-3}	1.94×10^{-4}	100	100

Table 3. Parameters of 6 MV photon beam of the experiment data compared to Gate 9.0 MC simulation

Field (cm ²)	Parameters	Measured data	Gate MC Simulation	Error estimation
3×3	D ₁₀ (%)	62.06	62.6791	0.6191 %
	d _{max} (mm)	15	15.5	0.0333 %
	d ₈₀ (mm)	58	57.5	0.0086 %
	OF	0.845	0.8512	0.0062 %
6×6	D ₁₀ (%)	65.59	65.0692	0.5208 %
	d _{max} (mm)	16	16	0 %
	d ₈₀ (mm)	62	62	0 %
	OF	0.948	0.9467	0.0013 %
10×10	D ₁₀ (%)	67.76	67.7956	0.0356 %
	d _{max} (mm)	15	15.5	0.0333 %
	d ₈₀ (mm)	66	66	0 %
	OF	1	1	0 %
	TPR _{20/10}	0.68846	0.682345	6.115 × 10 ⁻³ %
20×20	D ₁₀ (%)	70.54	70.2276	0.3124 %
	d _{max} (mm)	15	15.5	0.0333 %
	d ₈₀ (mm)	71	70.5	0.00704 %
	OF	1.03878	1.041284	0.25

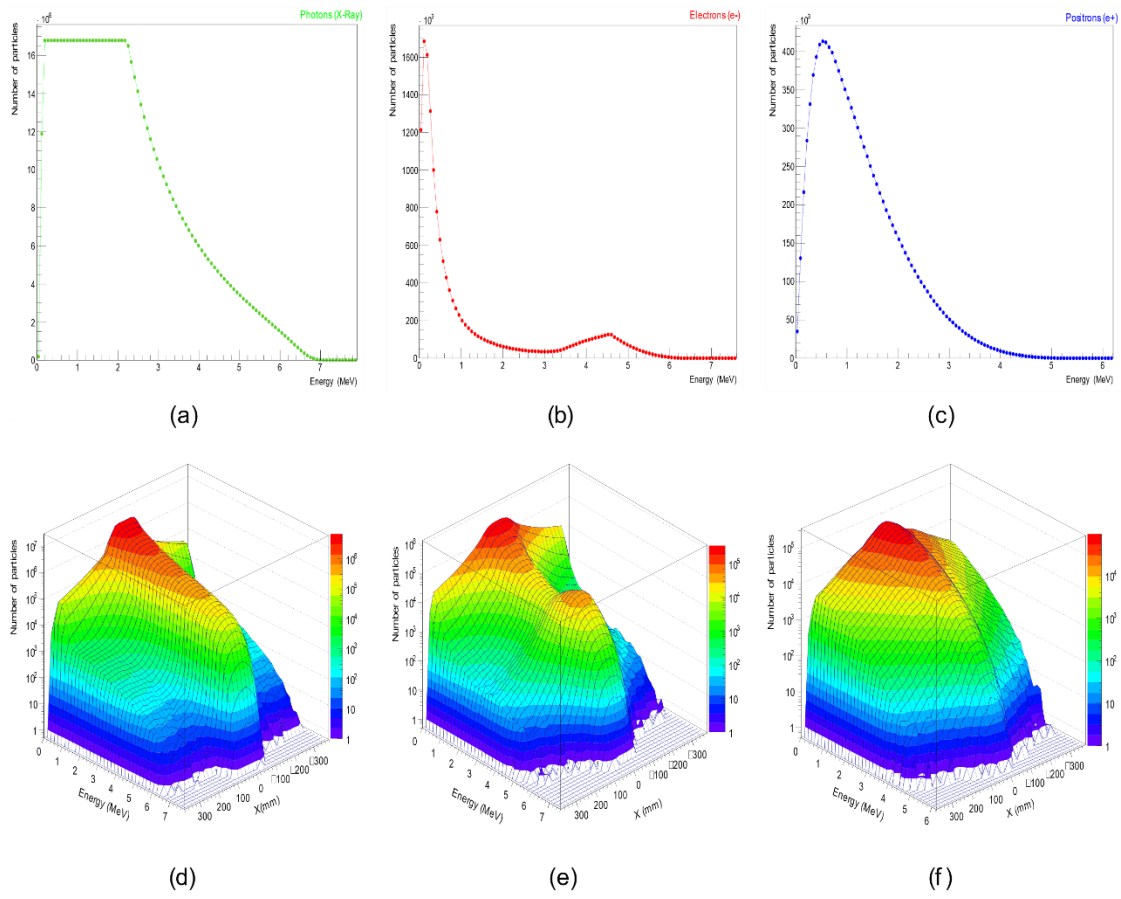


Figure 3. Correlation between coordinates of Python Phase Space. (a, b, c) represents the distribution of the energy spectrum of photons, e- and e+. (d, e, f) exhibits the distribution of X (mm) versus kinetic energy (MeV).

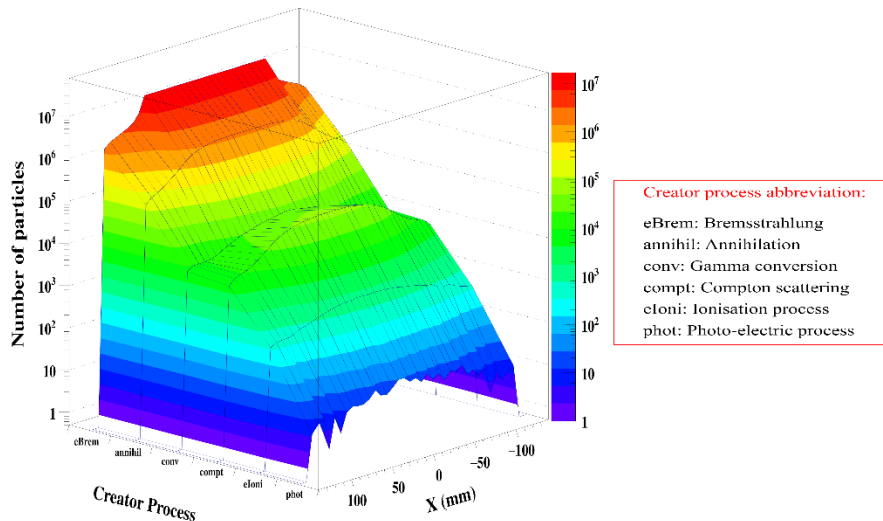


Figure 4. Creator process of particles (Photons, electrons, and positrons) versus the position X(mm) in the surface of Python phase space.

Analysis of the Python phase space

Figure 3 (a), (b) and (c) shows the spectral energy of particles scored in the phase space file. The mean energy of photons is 1.508 MeV with a distribution relatively flat from 0.1 to 2 MeV and a sharp fall-off from 2 to 6.7 MeV. The mean energy of electrons is 1.205 MeV with a distribution from 0 to 6 MeV. Additionally, the mean energy of positrons is 1.249 MeV with a distribution of spectral energy decreased gradually from 1 to 5 MeV.

The spatial distribution of each particle group as the function of kinetic energy is given in Figure 3 (d, e, f). This distribution represents an important parameter of the used model in this study to investigate the L&T of particles through the multi-leaf collimator MLCi2.

Figure 4 presents the number of particles related to the physical creator process names and position X where these physical processes were recorded in the Python phase space's plan surface. It is clearly seen that most particles are primary photons (X-ray) produced by the bremsstrahlung process in the target with a percentage of 86.3% of total particles. The scattered particles originate mainly from the primary collimator and the flattening filter. These components are responsible for the production of 13.7% of total particles. These results are in good agreement with the obtained results by Sheikh-Bagheri [20].

It enables precise authentication of the photon beam's quality [19]. The dissimilarity between the results from the MC Gate simulation and experiment at this comparison, as shown in Table 3, is less than 1.54%.

Analysis of the Python phase space

Figure 3 (a), (b) and (c) shows the spectral energy of particles scored in the phase space file. The mean energy of photons is 1.508 MeV with a distribution relatively flat from 0.1 to 2 MeV and a sharp fall-off from 2 to 6.7 MeV. The mean energy of electrons is 1.205 MeV with a distribution from 0 to 6 MeV. Additionally, the mean energy of positrons is 1.249 MeV with a distribution of spectral energy decreased gradually from 1 to 5 MeV.

The spatial distribution of each particle group as the function of kinetic energy is given in Figure 3 (d, e, f). This distribution represents an important parameter of the used model in this study to investigate the L&T of particles through the multi-leaf collimator MLCi2.

Figure 4 presents the number of particles related to the physical creator process names and position X where these physical processes were recorded in the Python phase space's plan surface. It is clearly seen that most particles are primary photons (X-ray) produced by the bremsstrahlung process in the target with a percentage of 86.3% of total particles. The scattered particles originate mainly from the primary collimator and the flattening filter. These components are responsible for the production of 13.7% of total particles. These results are in good agreement with the obtained results by Sheikh-Bagheri [20].

Leakage and Scattered Particles from MLC and Jaws (X, Y)

The results of the phase space plan located after the MLC are presented in Figure 5 and 6. Moreover, Figure 5 (a, b, c) shows the inter-leaf transmission, between-leaf and leaf-ends leakage for photons.

Figure 7 display scattered particles' energy spectra and mean energy in the function of radius distribution. The results have confirmed that the percentage of scattered particles increases in terms of field size (Figure 8 (a)) and could be modeled by an exponential function $F(x)$ (Equation 1). Furthermore, Figure 8 (b) displays the estimated rate value for a particular radiation field that describes the fraction of particles scattered from the MLCi2 and detected by the scoring plane normalized to the whole number of particles. The total amount of scattered radiation achieved for this investigation is under 0.2 %.

$$F(x) = TMath :: Exp(Slope[0].x + C^{st}) \rightarrow \begin{cases} Slope[0] = 0.12251 \pm 0.0056 \\ C^{st}[1] = -4.20112 \pm 0.1032 \end{cases} \quad (1)$$

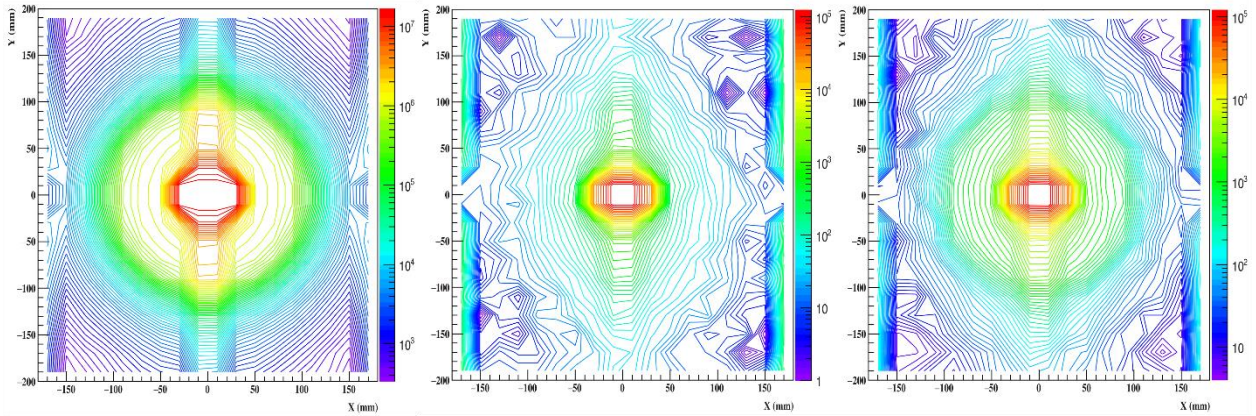


Figure 5. Spatial distribution of leakage particles (a) (b) and (c) of photons, electrons (e-) and positrons (e+) respectively.

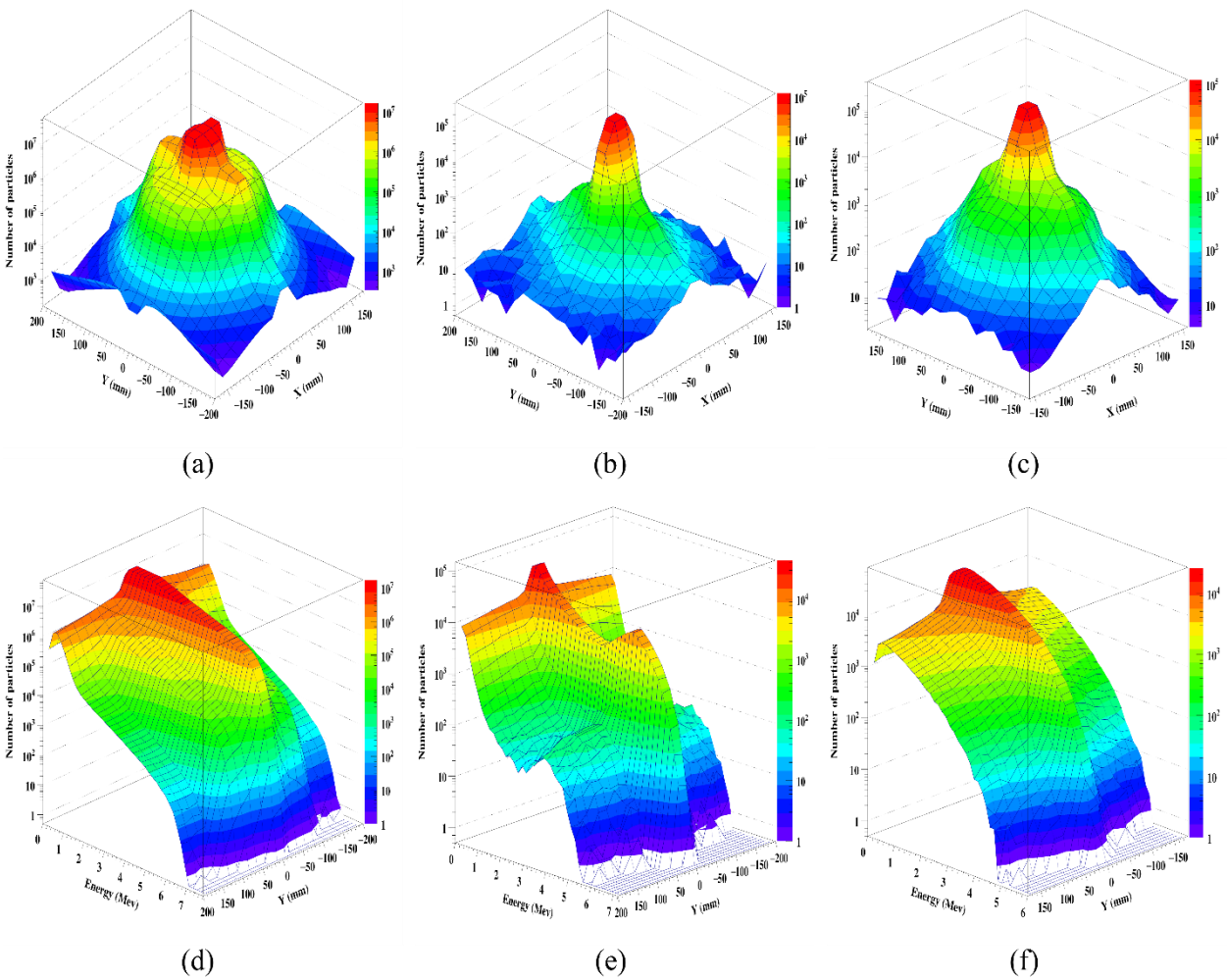


Figure 6. (a) spatial and kinetic energy distribution of leakage and transmitted photons (X-ray) (a, d), electrons (b, e) and positrons (c, f).

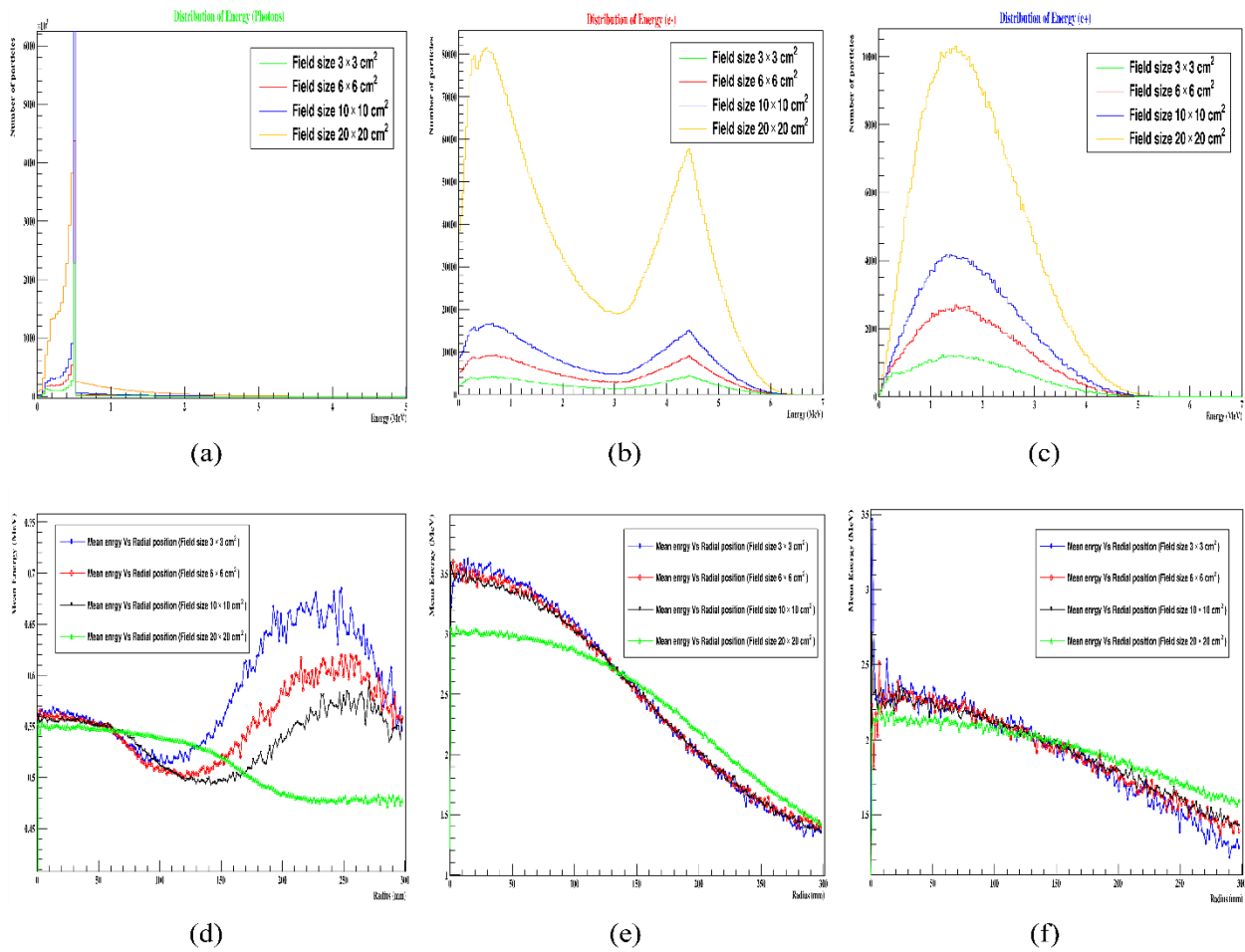


Figure 7. Energy spectra and the mean energy distribution in function of radius of scattered particles for Elekta Synergy 6 MV beams. Photons; (a, d); electrons; (b, e); positrons (c, f).

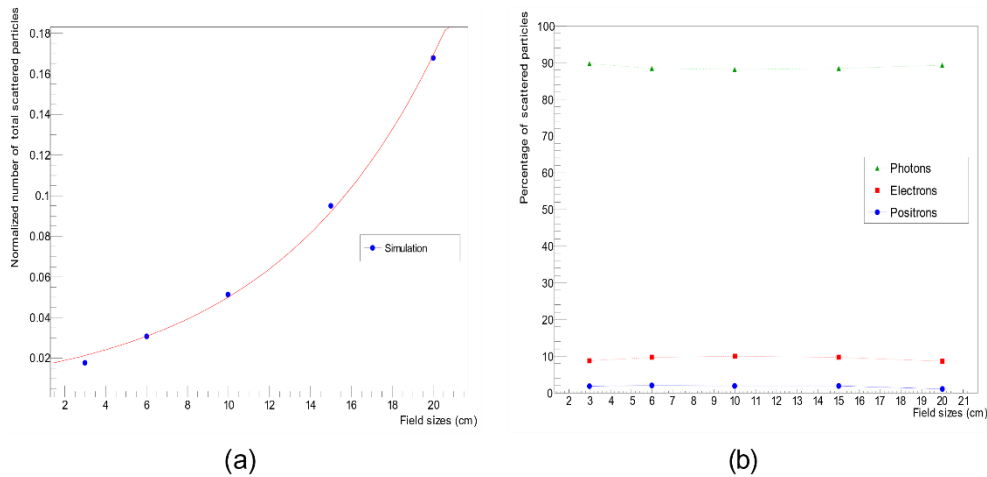


Figure 8. (a) The normalized total percentage of secondary collimator scatter particles in terms of field size for the Elekta Synergy 6 MV MLCi2, fitted using Equation (1). (b) The percentage of scattering photons, electrons, and positrons as a function of field size.

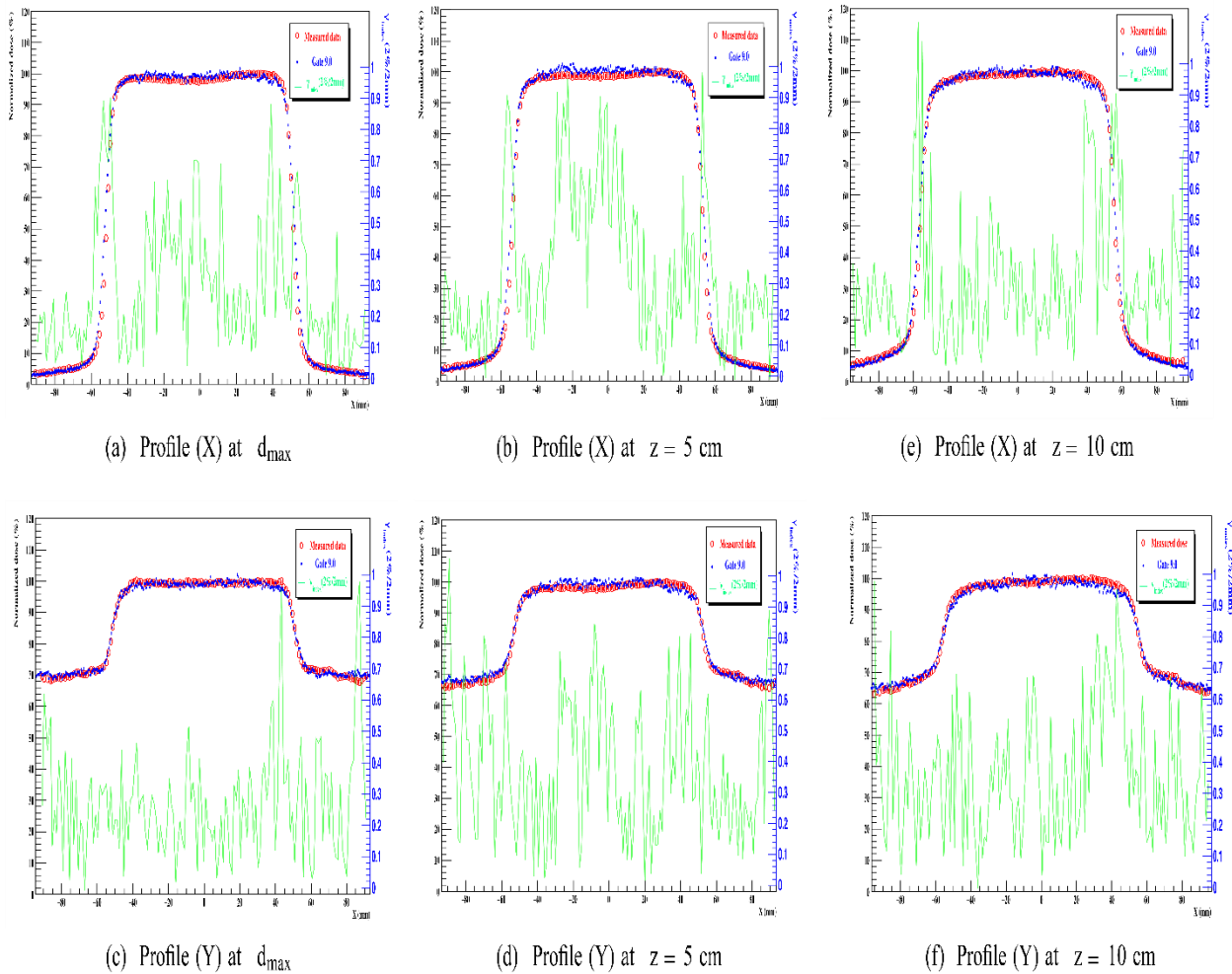


Figure 9. Comparison of simulated and measured profiles applying gamma index (2%/2mm) criteria for field size $10 \times 10 \text{ cm}^2$ without Jaws XY for 6 MV Elekta Synergy MLCi2 linac.

Dosimetric Study of LT radiations

In Figure 9, we show normalized cross profile's dose distribution for the field size $10 \times 10 \text{ cm}^2$ without the use of Jaws (X, Y), at $z = d_{\text{max}}$, 5 and 10 cm of depth for experimental and MC simulation applying Gate. Figure 9 also shows the gamma index (2%/2mm) distribution. It can be achieved that the cross profiles of the MC simulation (blue curves) are very matched with the measured data (red curve).

Dose distribution analysis in table 4 shows a good agreement for the small depth, to the deepest field at 10 cm, more than 98.72% and 99.34% of points have achieved the criteria 2%/2mm of simulation of cross profiles in X and Y axis, respectively. Unless the evaluation concerning Gate

simulation of dose differences by the use of ϵ and ϵ_{max} for cross profiles in X-axis indicated an error less than 3.026×10^{-3} and 8.101×10^{-3} , respectively. Besides, cross-profile in Y-axis evaluations registered an error less than 4.98×10^{-4} and 4.008×10^{-3} , respectively. Moreover, the average Distance to Agreement DTA value is limited to 0.2 mm, which is clinically satisfactory.

Therefore, Figure 10 shows a complex field composed of three small field sizes of $5 \times 5 \text{ cm}^2$. In this fact, the backup XY are used; despite everything, the organs at risk OARs between the irradiated areas is received 70% of the dose prescript to the Planning Target Volume PTV. These results are in perfect accordance with the achieved results by Kantz Steffi [21].

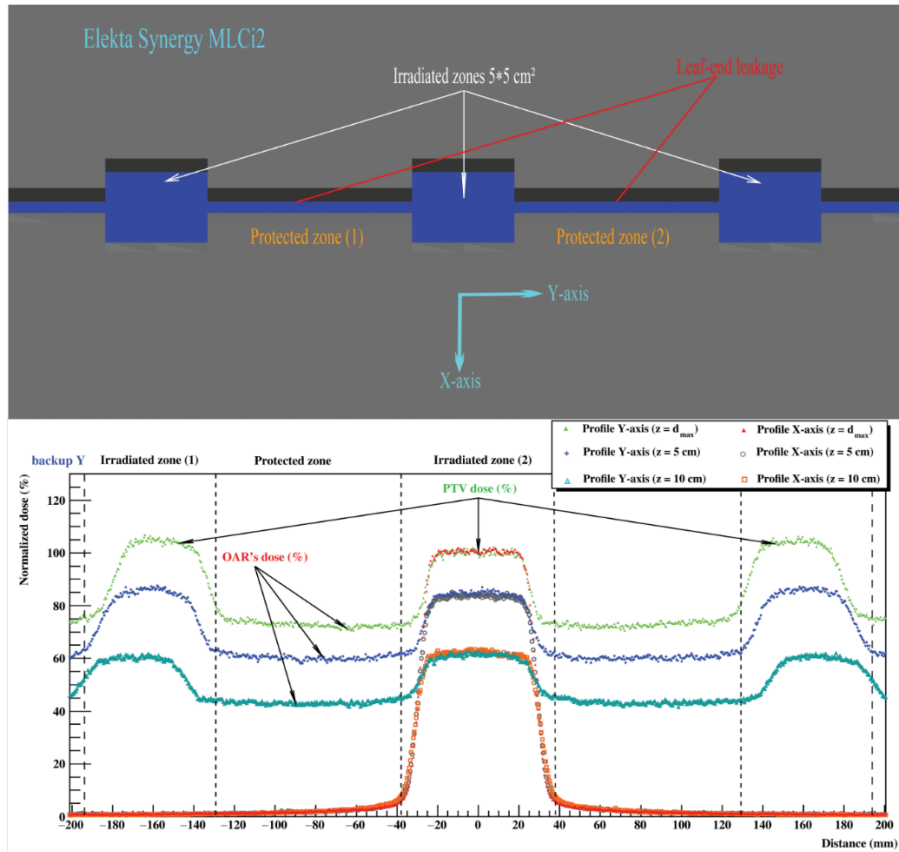


Figure 10. Dose distribution cross profiles in X-axis and Y-axis of a complex plan treatment composed of three sub-fields of size 5x5 cm².

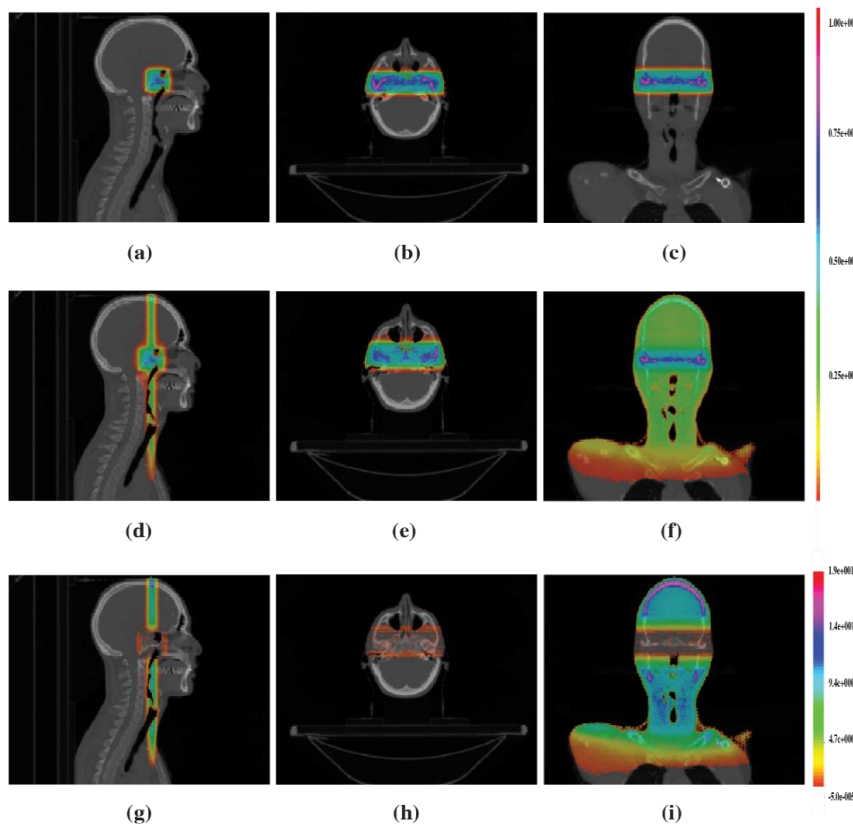


Figure 11. (a, b, c) treatment plan study with backup XY. (d, e, f) treatment plan study without backup XY. (g, h, i) distribution of gamma index (2%/2mm) in CT-Scan.

Table 4. Cross profiles simulation compared to measure experimentally at three depths d_{max} , 5 and 10 cm without the use of Jaws XY.

Depth (cm)	Profile (X) axis				Profile (Y) axis			
	ϵ	ϵ_{max}	$\gamma(2\%/2mm)$	DTA (mm)	ϵ	ϵ_{max}	$\gamma(2\%/2mm)$	DTA (mm)
Z = d_{max}	3.009×10^{-3}	7.531×10^{-4}	100	0.1	2.81×10^{-4}	2.38×10^{-4}	100	0.1
Z = 5 cm	2.957×10^{-3}	8.101×10^{-4}	100	0.1	3.95×10^{-4}	3.36×10^{-4}	99.3464	0.125
Z = 10 cm	3.026×10^{-3}	7.470×10^{-4}	98.7261	0.125	4.98×10^{-4}	4.008×10^{-4}	100	0.125

Figure 11 shows the dose distribution in three dimensions using a head CT image [22], applying two treatment plans composed of backup and without backup XY. Gamma index (2%/2mm) criteria in three dimensions are used to study the variation between treatment plans practiced in this investigation.

Discussion

The assessment of dose differences is shown in Table 2 using the metrics ϵ and ϵ_{max} , which represent the global gamma index and the maximum global gamma index, respectively. PDDs showed errors extending from 9.25×10^{-5} to 1.66×10^{-3} using the global ϵ index and 1.82×10^{-5} to 1.1×10^{-3} using the maximum global ϵ_{max} index. Additionally, the cross-profile assessments revealed errors ranging from 1.82×10^{-3} to 1.05×10^{-2} and 1.946×10^{-4} to 2.941×10^{-3} applying the global ϵ and the maximum global ϵ_{max} indexes, respectively. According to the local gamma index analysis γ_{index} carried out for PDD curves at the central beam axis, at least 100% and 99% of points passed the test for, respectively, 3%/2mm and 2%/2mm criteria. Analysis of the cross profiles reveals an almost continuous average percentage of points higher than 99% and 100% pass the test γ_{index} for 2%/2mm and 3%/2mm criterion, respectively, as a function of depth. In order to evaluate the accuracy at depth $z = d_{max}$, the locale gamma index displays more than 99% of the points have $\gamma(2\%/2mm) < 1$, and 100% have $\gamma(3\%/2mm) < 1$. These results indicate the high accuracy at d_{max} depth, where energy fluence fluctuations are large.

According to Figure 3, the distribution of photons, electrons and positrons can be described by cones with different radius. Figure 3 (d) explicates that most photons are regrouped inside a cone limited in 150 mm of radius, with a distribution of energy extending from 0.1 to 6.7 MeV. It can be concluded that this amount of photons can represent the primary photons arriving from the target. The rest of the distributed photons within the interval ranging from 150 to 400 mm (also -150 to -400 mm) can describe the scattered or secondary photons with a different arrangement in terms of energy spectrum characterized by a minimum equivalent to 0.1 MeV and a maximum equal to 5.5 MeV. Furthermore, according to Figure 5 more photons transmitted from the MLCi2 (Green cone with radius 120 mm) compared to electrons and positrons. This phenomenon can present photons' capability to be transmitted between-leaf without any interaction because of the small probability of interaction with mater compared to electrons and positrons. These findings are validated by Figure 6,

which shows that as the location Y (mm) in the MLC region rises from the center to the boundary, the number of electrons and positrons drops by 95%. Moving from the center of the MLCi2 volume to the edge, however, the proportion of photons drops slightly compared to (e-) and (e+), with an 88% proportion. As a result, many transmitted photons compared to the electrons and positrons, are observed around the central axis and decreases as one moves away from the center.

Based on Figure 9, the cross-profile distribution of dose in the X-axis compared with dose distribution in the Y-axis, show a remarkable difference, around 70% of the dose, which is delivered outside the scope of the target volume (opening of the field size), indicates that jaws XY can more protect the normal tissues. Nevertheless, in complicated shape tumors treatment, the jaws XY effect is restricted to the latest open MLCi2 leaf. A similar result of leakage particles achieved in two dimensions dose distribution is displayed for the examined fields in a three-dimension CT patient scan. Around 70% of the dose prescribed to the PTV is delivered to the OARs outside the field area definition. The percentage of points fails to satisfy the 3D gamma index 2%/2 mm criterion are over the whole field size. This deviation is due to leaf-end leakage particles outside the field size in the Y-axis.

Conclusion

To improve dose accuracy, this study demonstrates various particles' interactions with the Elekta Synergy MLCi2 linac components, as well as the fluency of the patient-dependent section segments. The calculating grid based on the High-Performance Computer (Slurm cluster) and the MC Gate 9.0 software are used to achieve this objective. The energy spectrum of every particle that originates from the Elekta Synergy MLCi2 Independent Patient Part is extracted using the Python phase space approach. It has been discovered that electrons and positrons significantly contribute to the X-ray photon field generated by Elekta Synergy MLCi2 linac. This contribution could be sufficient to have an impact on the dose that is administered to the patient. The accuracy of the suggested simulation model is confirmed by the quality of the results obtained for the studied parameters when compared to the experimental data. According to the validation tests performed for this work, the findings display a high agreement of 99% between the MC Gate 9.0 simulation and the experimental dose distributions. The rounded leaf ends bring a higher leakage of around 70% of the dose delivered to the tumor, applying the Elekta Synergy MLCi2 collimator. Any errors affecting the leaf position

precision in the process of movement, such as an incomplete closure, will increase the L&T. Therefore, the purpose of the backup XY is crucial for simple treatment plans, hence the periodic maintenance and check on the backup XY should be encouraged.

References

- Zheng Y, Qiu Y, Lu P, Chen Y, Fischer U, Liu S. An improved on-the-fly global variance reduction technique by automatically updating weight window values for Monte Carlo shielding calculation. *Fusion Engineering and Design*. 2019 Oct 1;147:111238.
- Lárraga-Gutiérrez JM, de la Cruz OG, García-Garduño OA, Ballesteros-Zebadúa P. Comparative analysis of several detectors for the measurement of radiation transmission and leakage from a multileaf collimator. *Physica Medica*. 2014 May 1;30(3):391-5.
- Krim DE, Rrhioua A, Zerfaoui M, Bakari D, Oulhouq Y, Bouta M. Simulation of the patient-dependent part 6 MV Elekta linac photon beam using GATE. In 2019 International Conference on Intelligent Systems and Advanced Computing Sciences (ISACS). 2019 : 1-6. IEEE. Doi: 10.1109/ISACS48493.2019.9068922.
- Gardner M, McNabb A, Seppi K. A speculative approach to parallelization in particle swarm optimization. *Swarm Intelligence*. 2012 Jun;6(2):77-116.
- Kim JO, Siebers JV, Keall PJ, Arnfield MR, Mohan R. A Monte Carlo study of radiation transport through multileaf collimators. *Medical physics*. 2001 Dec;28(12):2497-506.
- Arnfield MR, Siebers JV, Kim JO, Wu Q, Keall PJ, Mohan R. A method for determining multileaf collimator transmission and scatter for dynamic intensity modulated radiotherapy. *Medical physics*. 2000 Oct;27(10):2231-41.
- Li J, Zhang XZ, Gui LG, Zhang J, Tang XB, Ge Y, et al. Clinical feasibility of leakage and transmission radiation dosimetry using multileaf collimator of ELEKTA synergy-S accelerator during conventional radiotherapy. *Journal of Medical Imaging and Health Informatics*. 2016 Apr 1;6(2):409-15.
- Almond PR, Biggs PJ, Coursey BM, Hanson WF, Huq MS, Nath R, et al. AAPM's TG-51 protocol for clinical reference dosimetry of high-energy photon and electron beams. *Medical physics*. 1999 Sep;26(9):1847-70.
- Sanz DE, Alvarez GD, Nelli FE. Ecliptic method for the determination of backscatter into the beam monitor chambers in photon beams of medical accelerators. *Physics in Medicine & Biology*. 2007 Feb 26;52(6):1647.
- Papadimitroulas P. Dosimetry applications in GATE Monte Carlo toolkit. *Physica Medica*. 2017 Sep 1;41:136-40.
- Antcheva I, Ballintijn M, Bellenot B, Biskup M, Brun R, Buncic N, et al. ROOT—A C++ framework for petabyte data storage, statistical analysis and visualization. *Computer Physics Communications*. 2009 Dec 1;180(12):2499-512.
- Apostolakis S, Allison J, Amako KA, Apostolakis, & Geant4 Collaboration. GEANT4—a simulation toolkit. *Nucl Instrum Methods Phys Res*. 2003;506(3):250-303.
- Low DA, Dempsey JF. Evaluation of the gamma dose distribution comparison method. *Medical physics*. 2003 Sep;30(9):2455-64.
- Van Dyk J, Barnett RB, Cygler JE, Shragge PC. Commissioning and quality assurance of treatment planning computers. *International Journal of Radiation Oncology* Biology* Physics*. 1993 May 20;26(2):261-73.
- Krim DE, Rrhioua A, Zerfaoui M, Bakari D. Development of a new Hybrid Virtual Source Model to simulate Elekta Synergy MLCi2 linac. *Radiation Measurements*. 2022 May 20:106780.
- HPC-Marwan. 2018. Available from: www.marwan.ma/index.php/services/hpc.
- Krim DE, Rrhioua A, Zerfaoui M, Bakari D, Hanouf N. GATE Simulation of 6 MV Photon Beam Produced by Elekta Medical Linear Accelerator. In *International Conference on Electronic Engineering and Renewable Energy*. 2020: 301-7.
- Krim DE, Bakari D, Zerfaoui M, Rrhioua A. Implementation of a new virtual source model in Gate 9.0 package to simulate Elekta Synergy MLCi2 6 MV accelerator. *Biomedical Physics & Engineering Express*. 2021 Jul 8;7(5):055004.
- Musolino SV. Absorbed dose determination in external beam radiotherapy: an international code of practice for dosimetry based on standards of absorbed dose to water. *technical reports series*. 2001;398.
- Sheikh-Bagheri D, Rogers DW. Monte Carlo calculation of nine megavoltage photon beam spectra using the BEAM code. *Medical physics*. 2002 Mar;29(3):391-402.
- Kantz S, Söhn M, Troeller A, Reiner M, Weingandt H, Alber M, et al. Impact of MLC properties and IMRT technique in meningioma and head-and-neck treatments. *Radiation Oncology*. 2015 Dec;10(1):1-5.
- Sarrut D, Bardès M, Bousson N, Freud N, Jan S, Létang JM, et al. A review of the use and potential of the GATE Monte Carlo simulation code for radiation therapy and dosimetry applications. *Medical physics*. 2014 Jun;41(6Part1):064301.